UNCLASSIFIED

Defense Technical Information Center
Compilation Part Notice

ADP011241

TITLE: Quantitative Comparison of Single-Beam Gradient-Force Optical Traps and Dual-Beam Optical Traps

DISTRIBUTION: Approved for public release, distribution unlimited

This paper is part of the following report:

TITLE: Optical Sensing, Imaging and Manipulation for Biological and Biomedical Applications Held in Taipei, Taiwan on 26-27 July 2000. Proceedings

To order the complete compilation report, use: ADA398019

The component part is provided here to allow users access to individually authored sections of proceedings, annals, symposia, etc. However, the component should be considered within the context of the overall compilation report and not as a stand-alone technical report.

The following component part numbers comprise the compilation report:
ADP011212 thru ADP011255

UNCLASSIFIED

Quantitative comparison of single-beam gradient-force optical traps and dual-beam optical traps

Z. H. Huang, D. S. Mehta, H. C. Huang, C. F. Wang, and A. Chiou*
Department of Electrical Engineering, National Dong Hwa University,
1, Sec.2, Da Hsueh Rd. Shou-feng, Hualien, Taiwan, R.O.C.

ABSTRACT

In this paper, we compare the performance of the single beam gradient-force trap (SBGFT) and the counter propagating dual-beam trap (CPDBT) quantitatively in terms of three performance parameters, namely, the transverse trapping efficiency, the width of the stable trapping zone, and the axial stiffness. Ray-Optics Model (for optical trapping of Mie particles) was used to obtain the numerical results. In the SBGFT, the particle is trapped in the vicinity of the focal spot of a strongly focused (N.A. ~ 0.65 to 1.3) laser beam by gradient forces in both the transverse and the axial directions. In the CPDBT, with the two counter-propagating beams often mildly focused (N.A. < 0.6), the particle is confined transversely by the transverse gradient forces of the two beams, and stabilized axially by balancing the scattering forces from the two beams. Depending on the separation between the two beam waists, there can be more than one stable trapping zones in the CPDBT. Qualitatively, one obvious key advantage of SBGFT is that it is very simple to implement. In contrast, the CPDBT requires précised alignment of the two beams. The latter, however, allows longer working distance and offers more degrees of freedom. The theoretical values of the aforementioned performance parameters for the CPDBT vary over a wide range because they depend on the distance between two beam waists. This extra degree of freedom in the CPDBT allows us to trade off one performance parameter against the others. We have also measured these performance parameters experimentally to verify the general trend predicted by the theoretical model.

Keywords: Single-beam gradient force trap (SBGFT), counter-propagating dual-beam trap (CPDBT), transverse trapping efficiency, axial stiffness, stable trapping zone.

***Correspondence: E-mail: aechiou@mail.ndhu.edu.tw:Tel:886-38-662-500, Fax: 886-38-662-300.**

In *Optical Sensing, Imaging, and Manipulation for Biological and Biomedical Applications*, Robert R. Alfano, Ping-Pei Ho, Arthur E. T. Chiou, Editors, Proceedings of SPIE Vol. 4082 (2000) • 0277-786X/00/$15.00

1. INTRODUCTION

Optical trapping and manipulation of micro-particles using the radiation pressure of counter-propagating laser beams was first discovered by Ashkin in 1970[1]. In 1986 Ashkin et al[2] demonstrated the optical trapping of dielectric particles using a single beam gradient force trap (or the so-called "optical tweezers"). Since then both experimental configurations, i.e., the single-beam gradient-force trap (SBGFT) and the counter-propagating dual-beam trap (CPDBT) have been applied for many applications in the field of biological and biomedical sciences[3-7], as well as in physics[8-20]. Optical traps are often characterized by the trapping force (or the trapping efficiency) in the transverse and the axial directions, and the size of the stable trapping zone. In this paper, we compare the performance of the SBGFT and the CPDBT quantitatively in terms of three performance parameters, namely, the transverse trapping efficiency, the width of the stable trapping zone, and the axial stiffness. Theoretical results were obtained for both configurations using the Ray-Optics model. The experimental results for maximum transverse trapping efficiency of the CPDBT are compared with the corresponding theoretical results and a fair agreement was found. In the following section the Ray-Optics model (for optical trapping of Mie particles) is introduced. In Section 3, numerical results for maximum transverse trapping efficiency (Q_{tr}), the width of axial trapping zone, and the axial stiffness for SBGFT and CPDBT are compared. Description of the experimental technique for CPDBT and comparison of experimental results with the corresponding numerical results are presented in Section 4. Our main results are summarized in Section 5.

2. THEORETICAL ANALYSIS BY RAY-OPTICS MODEL

The Ray-Optics Model for predicting the forces acting on a particle in an optical trap was first proposed by Ashkin in 1992[21]. This model is applicable when the particle size is much larger than the wavelength of the trapping light. According to this model, reflection and refraction of light at the surface of the particle give rise to two types of forces on the particle. Reflection gives rise to scattering force, or radiation pressure, which is proportional to the optical intensity and points in the direction of propagation of the light beam. Refraction gives rise to a gradient force due to an optical intensity gradient and points towards the direction of increased intensity. Figure 1(a) shows the scattering and the gradient forces exerted by a Gaussian beam on a spherical particle (for the case where the refractive index of the particle is higher than that of the surrounding medium), along with the contribution of force components from two constituent pencils of ray (Ray A and Ray B). Figure 1(b) represents the geometry for calculating the force due to the scattering of a single incident ray of power P by a dielectric sphere. The total force acting on the particle is given by the following expression[21]

$$F_{tot}=F_s+iFg$$

$$= \frac{nP}{c}\left[1+R\cos 2\theta\right]+i\frac{nP}{c}R\sin 2\theta-\frac{nP}{c}T^2\sum_{n=0}^{\infty}R^n e^{i(a+nb)} \tag{1}$$

where the scattering force F_s and the gradient force F_g acting on the particle are given by

$$F_s=\frac{nP}{c}\left\{1+R\cos 2\theta-\frac{T^2\left[\cos(2\theta-2\theta_r)+R\cos 2\theta\right]}{1+R^2+2R\cos 2\theta_r}\right\} \tag{2}$$

$$F_g=\frac{nP}{c}\left\{R\sin 2\theta-\frac{T^2\left[\sin(2\theta-2\theta_r)+R\sin 2\theta\right]}{1+R^2+2R\cos 2\theta_r}\right\} \tag{3}$$

In equations (2) and (3), n is the refractive index of the surrounding medium, P is the laser beam power, c is the speed of light, R is the reflectance of light at the surface of the particle, T is the transmittance of light, θ is the angle of incidence, and θ_r is the angle of refraction. The total force on the sphere (Fig. 1(b)) is the sum of the contributions due to the reflected ray of power PR and infinite number of emergent refracted rays of successively decreasing power PT^2, PT^2R,....PT^2R^n,...[21]. The total scattering force F_s, the gradient force F_g, and the absolute magnitude of the total force $F_{mag}=(F_s^2+F_g^2)^{1/2}$ can be calculated as function of the angle of incidence θ using equations (1) and (2), and the corresponding trapping efficiencies Q_s, Q_g, and $Q_{mag}=(Q_s^2+Q_g^2)^{1/2}$ can be calculated using the following expression[21]

$$F=Q(nP/c) \quad (4)$$

where Q represents the optical trapping efficiency and the quantity (nP/c) is the incident momentum per second of a ray of power P in a medium of refractive index n. The trapping force can be measured by balancing against a dragging force in a viscous fluid, and by using Stokes Law, $F_D=6\pi\eta rv$, where F_D is the dragging force, η = 0.001025Ns/m^2 is the viscosity of water, r is the radius of the sphere, and v is the critical velocity, which is defined as the velocity at which the sphere escapes from the optical trap due to the viscous drag.

3. NUMERICAL RESULTS

In this section the numerical results for aforementioned parameters are presented for both configurations. The parameters used in the calculations are, laser beam power, (10mW for SBGFT, and 5mW each for CPDBT), wavelength of the laser (λ=532nm), particle size (15μm), and surrounding refractive index (n=1.33). The total scattering force (F_s) and total gradient force (F_g) were computed using Eqs. (2) & (3) and the total trapping force on the micro-sphere was computed using Eq. (1). The transverse trapping efficiency (Q_{tr}) was evaluated from equation (4) using these data. The results are presented in the following sub-section.

3.1 Transverse trapping efficiency

The maximum transverse trapping efficiencies were calculated for SBGFT using objectives with NA varying from 1.25 to 0.65, and as a function of beam waist separation d, for CPDBT using a low numerical aperture objective (NA=0.40). The theoretical results are shown in Fig. 2. From this figure we see that the maximum transverse trapping efficiency (Q_{tr}) of CPDBT, at the beam waist separation d=0, is higher than that of the SBGFT and that Q_{tr} of CPDBT covers a wide range of values as compare to Q_{tr} of SBGFT. It can also be seen that the transverse trapping efficiency of the dielectric particle decreases on increasing the value of NA of the trapping objective in the case of SBGFT. Experimentally, we have also observed that the axial trapping force of the SBGFT is, in general, greater than that of the CPDBT. In the case of CPDBT a shorter beam waist separation, d, and a larger relative refractive index result in a stronger transverse confinement of the particle[15].

3.2 The axial trapping zone width

Figure 3 shows the results of the calculations of axial trapping zone width for CPDBT and SBGFT. In the CPDBT, the particle is confined transversely to the common beam axis by the transverse gradient forces of two weakly focussed laser beams. The particle is stabilized axially at a location where the scattering forces of two beams balance each other and also at the two beam waists. Therefore the CPDBT has a larger trapping zone width than SBGFT. Besides, the trapping position along the axis of the beams can be easily adjusted, in the case of CPDBT, by changing the relative intensity of the two laser beams. On the other hand, in the SBGFT, the beam is strongly focussed to a diffraction-limited spot by a high-numerical aperture objective and a strong three-dimensional gradient-force trap is created in the vicinity of the focus point and hence has only one stable trapping zone. It can also be seen from the Fig.3 that the width of axial trapping zone decreases on increasing the value of NA of the objective in the case of single-beam trap. The trapping zone width is, for example, about 13μm in a single beam trap (with NA=1.25, laser power = 10mW, and particle size = 15μm).

3.3 The axial stiffness

In a stable 3D-optical trap, the axial stiffness is an important parameter that dictates the resolution of the optical trap as a force-transducer for the measurement of force (typically on the order of pico-Newton). For small displacements from the center of the optical trap, the restoring force is proportional to displacement, i.e. the optical tweezers act like a linear spring obeying Hook's law. There are various methods to determine axial stiffness, such as the escape force method, the drag force method, and the equi-partition method[13]. We used drag force method to measure the axial stiffness for CPDBT and SBGFT. By applying a known viscous drag force, F, and measuring the displacement produced from the trap center, z, the axial stiffness can be determined by $F=\alpha z$; where α is the axial stiffness. The axial stiffness depends on various experimental parameters. We calculate the axial stiffness as a function of beam waist separation d, in the case of CPDBT, and for the values of NA (of the objective) varying from 0.65 to 1.25 in the case of SBGFT. Our results indicated that the SBGFT often provides a higher axial stiffness than the CPDBT.

The theoretical results of the axial stiffness for both cases are depicted in Fig.4. In the case of SBGFT, the axial stiffness increases on increasing the NA of the objective.

4. EXPERIMENTAL SETUP AND RESULTS FOR CPDBT

Figure 5 illustrates the basic experimental set-up for the CPDBT. A Nd:YAG laser (with a frequency doubler) of wavelength 532nm was used to generate the trapping beams. The laser light was expanded and collimated using a spatial filter and a beam expander (SF/BE) to a spot size of 1cm diameter. A set of half-wave ($\lambda/2$) plate and a polarizer was used for controlling the laser power and the polarization of the trapping beam. A relay lens of focal length 250mm was used to control the focus position of the trapping light. The expanded laser beam was devided by the polarizing beam splitter (PBS) and further directed by two beam splitters (BS) in counter-propagating directions along a common optical axis (as shown in Fig.5). Two microscope objectives (NA=0.45 each) were used to focus the counter propagating beams on the sample from the opposition directions. A glass capillary tube (with a square inner cross-section of 0.2 mm x 0.2 mm) filled with Polystyrene spheres of size 15μm in water was put in the focal point of the two counter propagating beams. The sample tube was mounted on a x-y-z motorized translation stage of 10μm/s velocity resolution, and 0.5μm position resolution. The laser beam power for trapping was 5mW each. A polarizer and a polarizing beam splitter (PBS) was used for changing the power ratio of two beams. An incoherent light source was used to illuminate the sample particles for imaging on a TV monitor using a CCD camera. The experimental arrangement on the right side of Fig. 5 shows the side view of the sample cell and the associated optics for observing the trapped particle from the top. Fig. 6 shows the image of a particle trapped by the CPDBT inside the capillary.

We measured the transeverse trapping force by dragging the tube (with a particle trapped in the beam) in the direction parallel to the tube axis using the motorized translation stage. The drag force (or the equivalent trapping force) was calculated from the measured escape velocity and the Stokes law. The experimental results were compared with the theoretical results obtained from the Ray-Optics Model. Figure 7 shows a comparison of the experimental data (points in Fig.7) and the theoretical results (solid line in Fig. 7) for the maximum transverse trapping efficiency $(Q_{tr})_{max}$ for the CPDBT. Although the general trend of the experimental results follows the theoretical curve, the detail differs. For example, the experimental values of Q_{max} peak at beam waist separation d = 14.2μm, while the corresponding theoretical values peak at beam waist separation d = 0, and distributed symmetrically around d = 0. The asymmetry (and the discrepancy) in the experimental values of Q_{max} is probably due to the imperfection in the alignment. Moreover, the theoretical results for Q_{max} were calculated particle trapped in the π_M –plane shown in Fig.2, whereas in actual practice, the particle may not be stabilized exactly in the π_M – plane; hence, the discrepancy may also be attributed to this factor.

5. SUMMARY

A theoretical analysis has been presented for CPDBT and SBGFT in terms of three performance parameters, namely, the transverse trapping efficiency, the width of the stable trapping zone, and the axial stiffness. Ray-Optics Model (for optical trapping of Mie particles) was used to obtain the theoretical results. The theoretical results for SBGFT and CPDBT are summarized in table I.

Table I Quantitative comparison of transverse trapping efficiency, axial trapping zone width, and axial stiffness for SBGFT and CPDBT.

	SBGFT				CPDBT
NA	1.25	0.95	0.85	0.65	0.4
Transverse Trapping Efficiency (Q_{tr})	0.281	0.375	0.392	0.415	From 0 - 0.431
Axial Trapping Zone Width (μm)	13	18	19	26	From 0 - 86
Axial Stiffness (pN/μm)	0.5	0.385	0.285	0.140	From 0 – 0.314

Each of the two experimental configurations has its own merit. The values of the three performance parameters for the CPDBT vary over a wide range because they depend on the separation between the two beam waists. This extra degree of freedom in the CPDBT allows us to trade off one performance parameter against the others. We have also measured experimentally the maximum transverse trapping efficiency (Q_{max}) in the case of CPDBT and compared with the corresponding theoretical results. The experimental data follow the general trend predicted by the theory.

ACKNOWLEDGEMENT

This project is supported by the National Science Council, Taiwan, under the Research Grant #NSC87-2112-M-259-002.

REFERENCES

1. A. Ashkin, "Acceleration and trapping of particles by radiation pressure", *Phys. Rev. Lett.* **24,** pp. 156-159 1970.
2. A. Ashkin, J. Dziedzic, J. Bjorkholm, S. Chu, "Observation of a single-beam gradient force optical trap for dielectric particles", *Opt. Lett.* **11,** pp. 288-290, 1986.
3. S. Sato, H. Inaba, "Optical trapping and manipulation of microscopic particles and biological cells by laser beams", *Opt. Quant. Electron.,* **28,** pp. 1-16, 1996.
4. A. Ashkin, J. M. Dziedzic, and T. Yamane, "Optical trapping and manipulation of single cells using infrared laser beams", *Nature* **330,** pp. 769-771, 1987.
5. K. Svoboda, S. M. Block, "Biological applications of optical forces", *Annu. Rev. Biophys. Biomol. Struct.* **23,** pp.247-285, 1994.
6. J. T. Finer, R. M. Simmons, and J. A. Spudich, "Single myosin molecule mechanics:piconewton forces and nanometer steps", *Nature* **368,** pp. 113-119, 1994.
7. C. M. Coppin, J. T. Finer, J. A. Spudich, and R. D. Vale, "Detection of sub-8-nm movements of kinesin by high-resolution optical-trap microscopy", *Proc. Natl. Acad. Sci. U.S.A.* **93** , pp. 1913-1917, 1996.
8. L. Malmqvist, and H. M. Hertz, "Trapped particle optical microscopy", *Opt. Comm.* **94,** pp.19-24, 1992.
9. L. Ghislain, W. Webb, " Scanning-force microscope based on an optical trap", *Opt. Lett.* **18,** pp.1678-1681, 1993.
10. S. Kawata, Y. Inouye, and T. Suguira, "Near-field scanning optical microscope with a laser trapped probe", Jpn. J. Appl. Phys. **33,** pp. L1725-L1727, 1994.
11. L. Malmqvist, M. Hertz, "Two-color trapped-particle optical microscopy",*Opt. Lett.* **19,** pp. 853-855, 1994.
12. M. E. J. Friese, H. Robinsztein-Dunlop, N. R. Heckenberg, and E. W. Dearden, "Determination of the force constant of a single beam gradient force trap by measurement of backscattered light", *Appl. Opt.* **35,** pp.7112-7116, 1996.
13. K. Visscher, S. P. Gross, and S. M. Block, "Construction of multiple-beam optical trapps with nanometer resolution position sensing", *IEEE J. of Selected Topics in Quant. Electr.* **2.** Pp. 1066-1076, 1996.
14. T. Suguira, T. Okada, Y. Inouye, O. Nakamura, S. Kawata, "Gold-bead scanning near-field optical microscope with laser force position control", *Opt. Lett.* **22,** pp.1663-1665, 1997.
15. E. Sidick, S. D. Collins, and A. Knoesen, "Trapping forces in a multiple-beam fiber-optic trap", Appl. Opt. **36,** pp. 6423-6433, 1997.
16. E. Fallman, and O. Axner, "Design for fully steerable dual-trap optical tweezers", Appl. Opt. **36,** pp. 2107-2113, 1997.
17. M. Gu, P. C. Ke, "Image enhancement in near-field scanning optical microscopy with laser trapped metallic particles", *Opt. Lett.* **24,** pp. 74-76, 1999.
18. P. C. Ke, and M. Gu, "Characterization of trapping force on metallic Mie particles", Appl. Opt. **38,** pp.160-167, 1999.
19. M. E. J. Friese, A. G. Truscott, H. Rubinsztein-Dunlop, N. R. Heckenberg, "Three-dimensional imaging with optical tweezers", *Appl. Opt.* **38** , pp. 6597-6603, 1999.
20. P. Zema'nek, A. Jonas, L. Sramek , M. Liska, "Optical trapping of nanoparticles and microparticles by a Gaussian standing wave", *Opt. Lett.* **24,** pp. 1448-1450, 1999.
21. A. Ashkin, "Forces of a single-beam gradient laser trap on a dielectric sphere in the ray optics regime", *Biophys. J.* **61,** pp. 569-582, 1992.

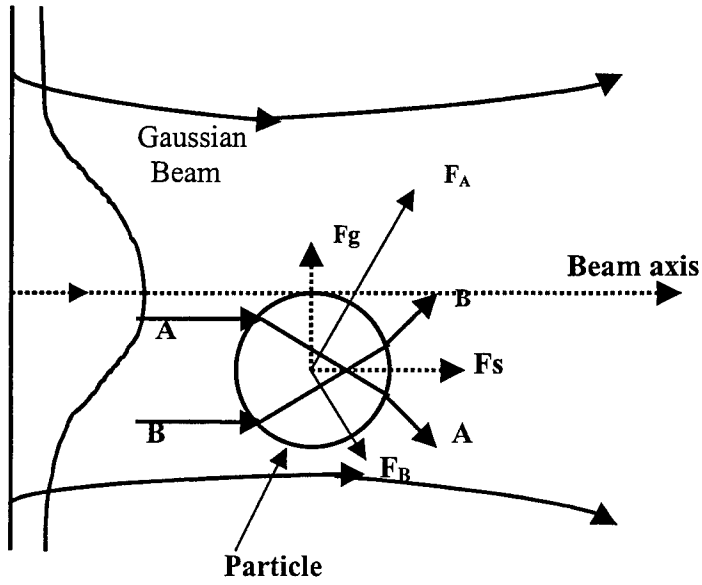

(a)

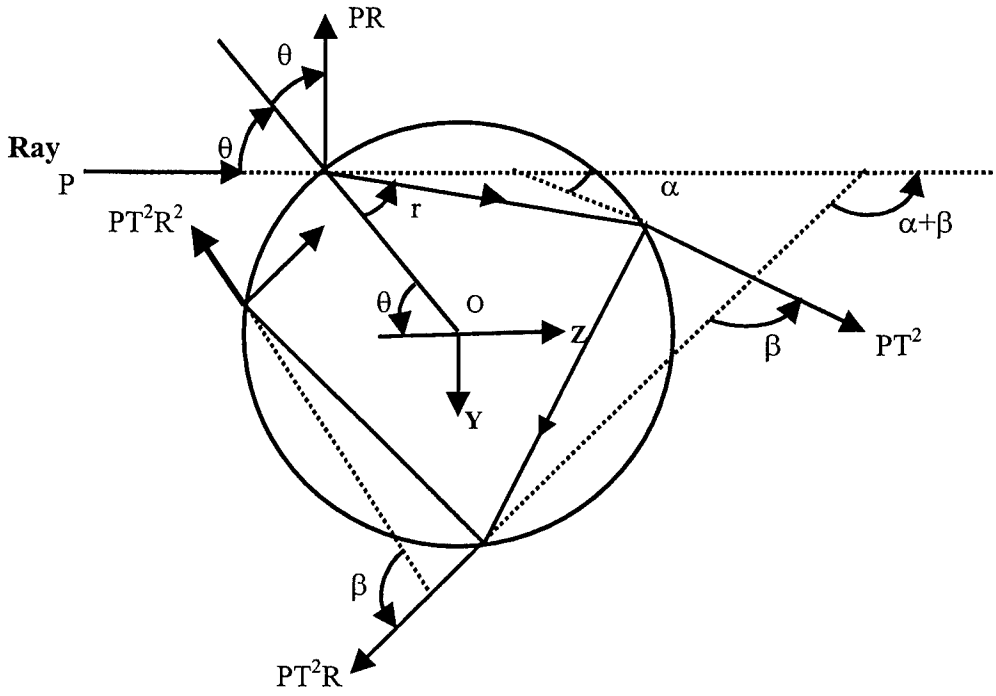

(b)

Fig. 1 (a) Geometry of Gaussian beam giving rise to the gradient force F_g and the scattering force F_s. (b) Geometry for calculating the force due to the scattering of a single incident ray of power P by a dielectric sphere.

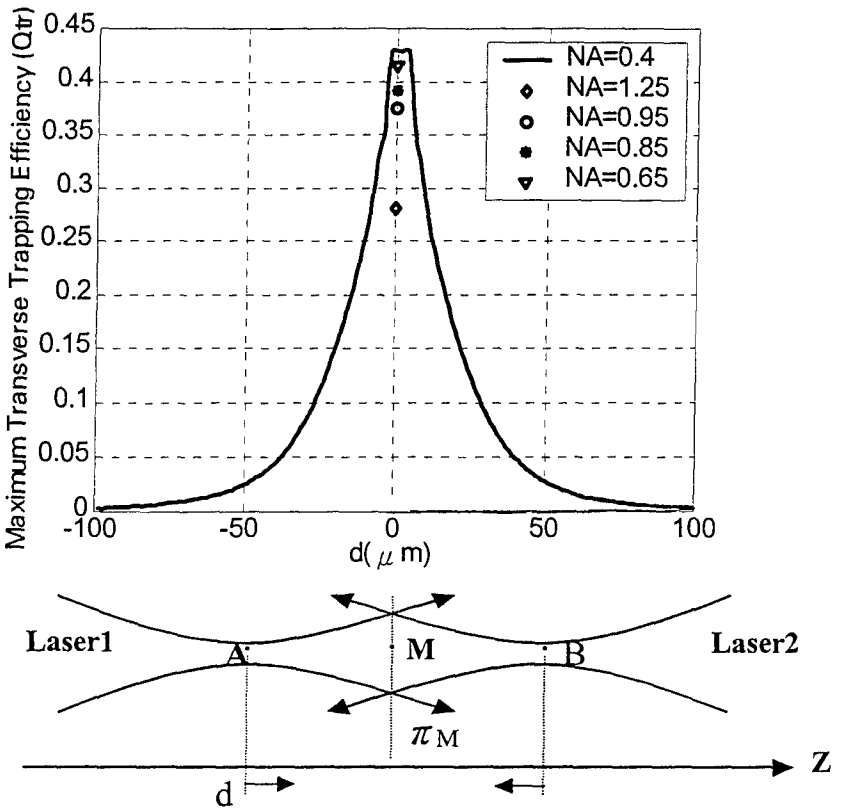

Fig. 2 Distribution of maximum transverse trapping efficiency (Q_{tr}) for CPDBT (solid line) as a function of the beam waist separation, and for SBGFT (dots) with various NAs.

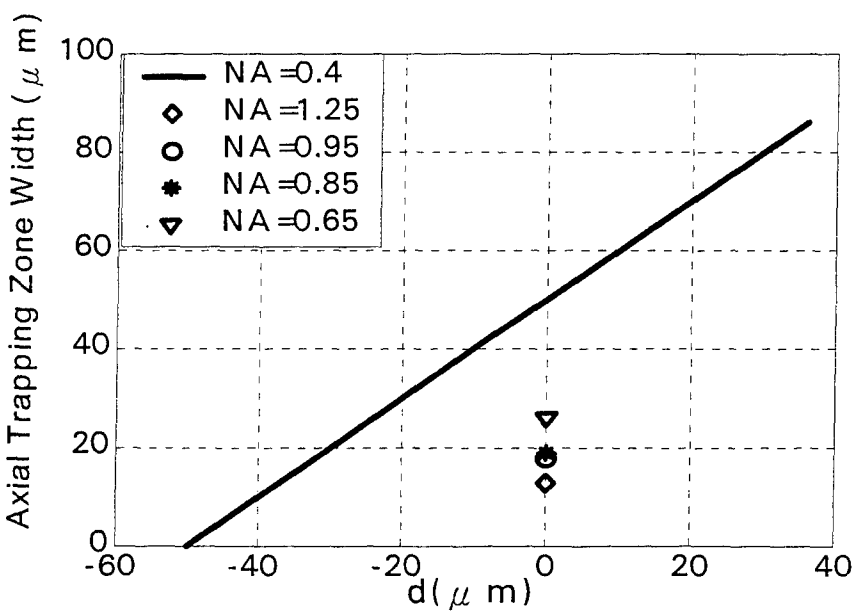

Fig. 3 Comparison of axial trapping zone width of CPDBT and SBGFT with respect to beam waist separation distance, d.

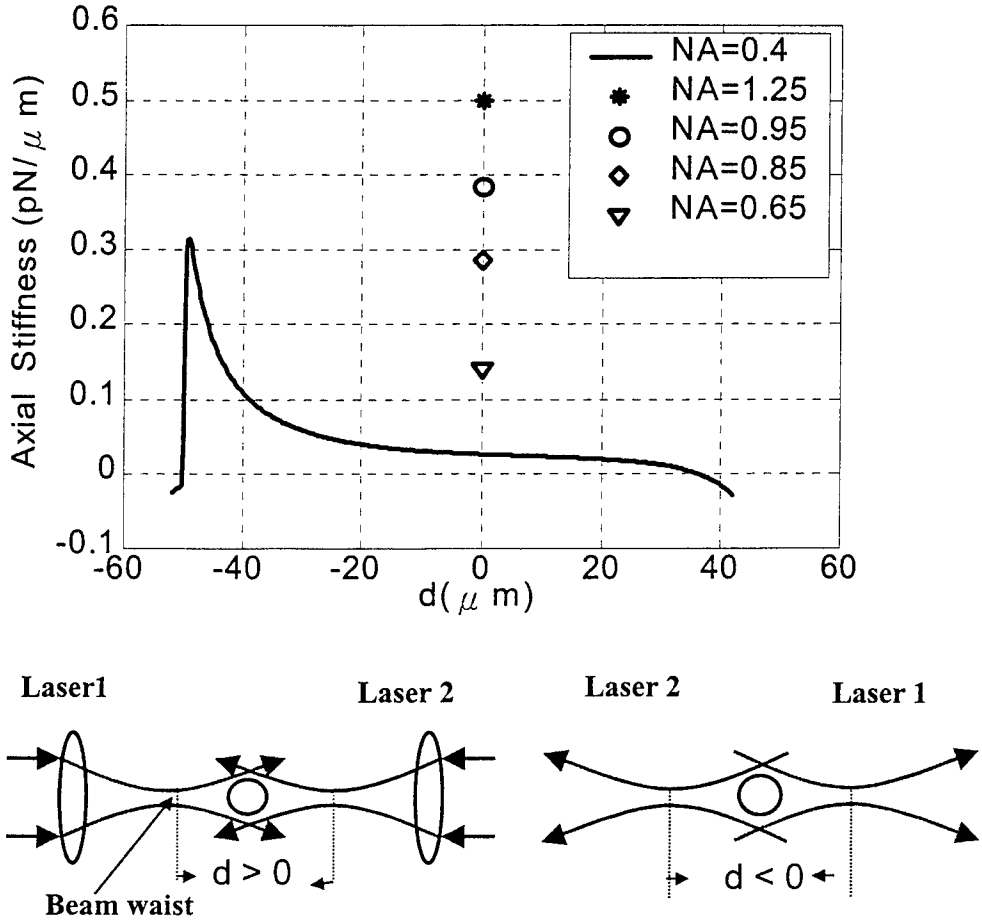

Fig. 4 Axial stiffness as a function of axial trapping position d for CPDBT (Solid line) and for SBGFT (symbols).

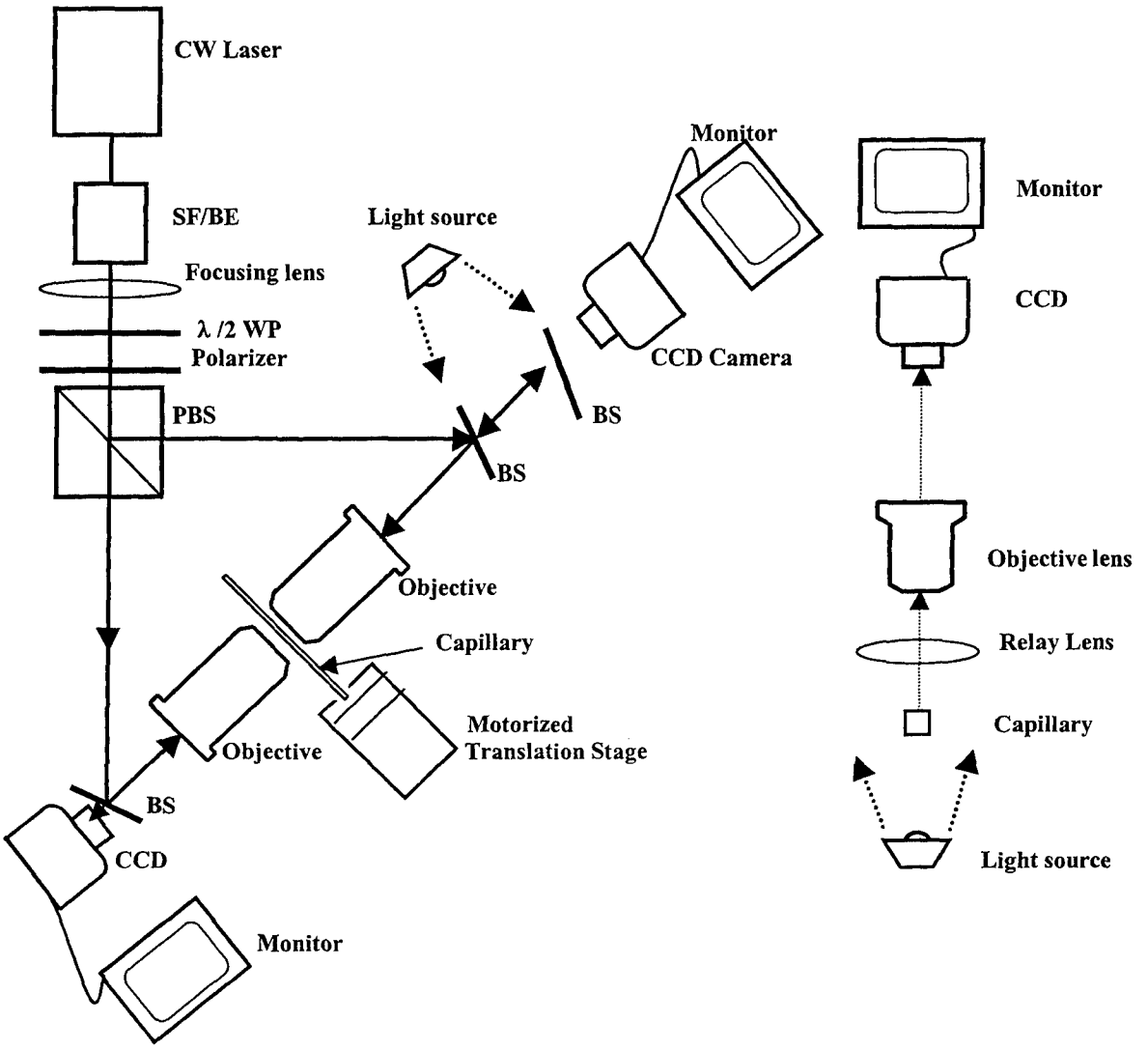

Fig. 5 Arrangement of the experimental setup for counter propagating dual beam trap (CPBDT).

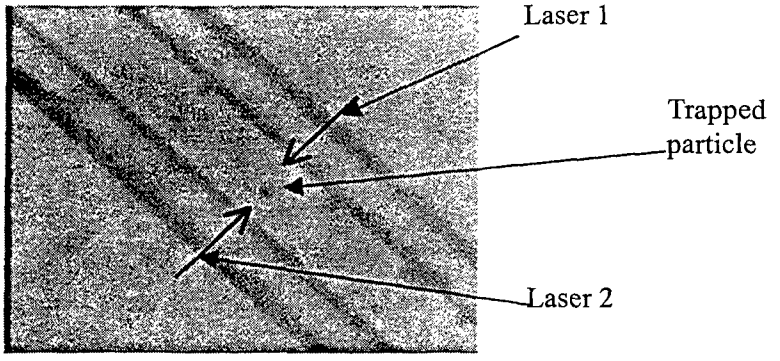

Fig. 6 Image of the trapped particle recorded by CCD camera under the bright field illumination.

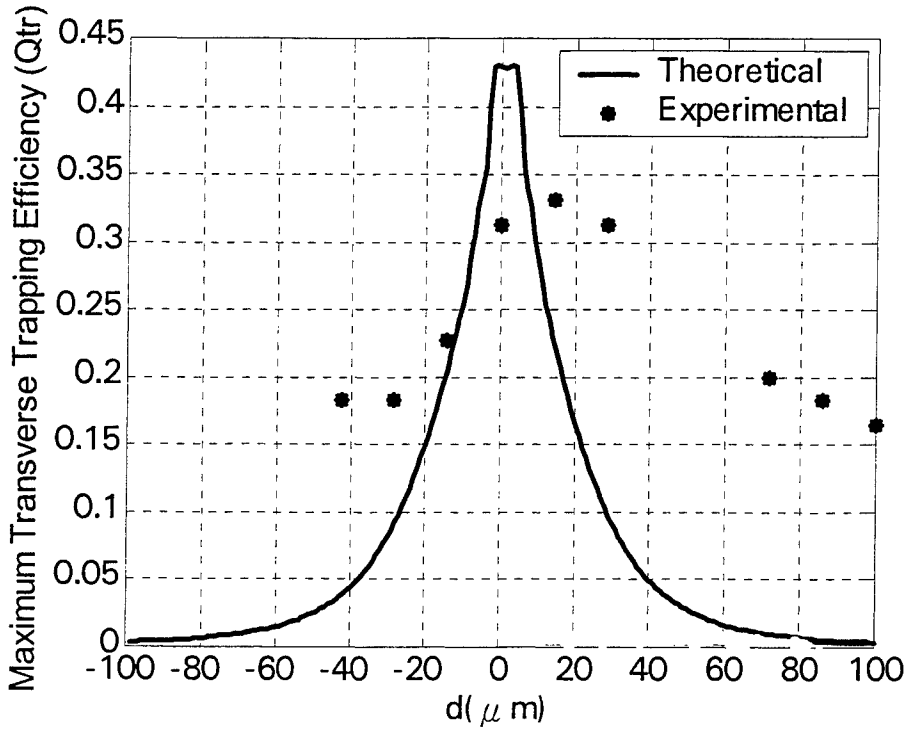

Fig. 7 Comparison of the experimental results with the theoretical results for transverse trapping efficiency for CPDBT.